Resonant Frequencies of Rectangular Microstrip Antennas with Flush and Spaced Dielectric Superstrates

Jennifer T. Bernhard, *Member, IEEE,* and Carolyn J. Tousignant, *Student Member, IEEE*

***Abstract*— This paper presents a predictive model for the resonant frequencies of rectangular microstrip antennas with flush and spaced superstrates. This closed-form model is suitable for CAD and is directly applicable for the integration of microstrip antennas beneath plastic covers or protective dielectric superstrates in portable wireless equipment. The model utilizes conformal mapping and the concept of equivalent capacitance to determine the effective permittivity of a covered microstrip structure. A comparison between calculated and measured resonant frequencies demonstrates that the model provides less than 1% errors for structures with low relative permittivities ($\varepsilon_r < 3$) and slightly higher errors for structures that contain higher permittivity materials. Generally, the model predicts the resonant frequency of a spaced superstrate structure as accurately as possible within the tolerance range of the structure's electrical and physical parameters.**

***Index Terms*—Microstrip antennas, resonant frequency, superstrates.**

I. Introduction

MICROSTRIP antennas are becoming a popular choice for a range of portable wireless equipment since they are light weight, low cost, and straightforward to design. Increasingly, however, these applications require that the antenna(s) be placed out of the sight of the consumer, beneath plastic covers or protective dielectric superstrates. Placement of such a dielectric cover over a microstrip antenna shifts the antenna's resonant frequency by changing the effective permittivity of the microstrip structure. Microstrip antennas designed without consideration of these frequency shifts will not perform as expected once installed in a portable unit.

Several researchers have addressed the effect of dielectric covers on effective permittivity and microstrip antenna characteristics, particularly resonant frequency. Bahl *et al.* [1] utilized a variational technique in the Fourier domain to describe the rectangular structure's effective permittivity, while Verma *et al.* [2] combined a similar variational technique with a transmission line model for the covered rectangular antenna. Shavit [3] and Fan and Lee [4] presented spectral domain analyses that examine the resonance and input impedance characteristics of covered microstrip antennas. Verma and Rostamy [5], Damiano and Papiernik [6], and Damiano *et al.* [7] also proposed modified Wolff models to calculate the resonant frequencies of various microstrip structures. Pozar [8], Mosig and Gardiol [9], Michalski and Zheng [10], and Ramahi and Lo [11] applied a method of moments approach to calculate antenna resonant characteristics. Also, Bhattacharyya and Tralman [12] developed empirical relationships between the antenna's resonant frequency, input impedance, and superstrate thickness through experiment. All of these efforts produced reasonably accurate results. However, none of these formulations are appropriate for direct integration into a computer-aided design (CAD) package due to their often high computational cost and complexity. Additionally, none account for any intentional or unintentional air gaps between the antenna and the superstrate.

Uniquely, Afzalzadeh and Karekar [13] have considered the effects of a spaced dielectric superstrate on a microstrip patch antenna. They concluded that the spaced superstrate has negligible effects on the resonant characteristics of the antenna as long as the air gap between the patch and the superstrate is at least a free-space wavelength. However, such large spacings between antennas and superstrates in an integrated portable package such as a handset or portable computer are impractical. Moreover, the authors report considerable shifts in resonant frequency for air gaps on the order of a tenth of a free-space wavelength.

This paper develops accurate design equations that predict the resonant frequencies of rectangular microstrip antennas with both flush and spaced dielectric superstrates. These closed-form equations are suitable for CAD. In addition, the equations provide clear relationships between antenna dimensions, material properties, and antenna resonance, creating the ability to analyze covered antenna behavior in terms of intuitive models [14]. This development improves and expands upon the work done by Wheeler [15], Svačina [16], and Zhong *et al.* [17] to include the effects of both intentional and unintentional air gaps between the antenna and the su-

Manuscript received October 8, 1997; revised March 31, 1998. This work was supported in part by the National Science Foundation under Grant ECS-9626599, National Science Foundation Research Experiences for Undergraduates (REU) under Grant CDA-9322248, and a University of New Hampshire Summer Faculty Fellowship.

J. T. Bernhard is with the Electrical and Computer Engineering Department, University of New Hampshire, Durham, NH 03824 USA.

C. J. Tousignant is with Raytheon Systems Company, Bedford, MA 01730 USA.

Publisher Item Identifier S 0018-926X(99)03726-6.

perstrate. In a manner similar to these researchers, we utilize conformal mapping and the concept of equivalent capacitance to determine the effective permittivity of a covered microstrip structure. This work includes the development of new filling fractions that rectify inconsistencies in previous work as well as the new arrangement of these filling fractions to reflect the true configuration of the electric flux in the multilayer structure. Our method predicts the resonant frequencies of covered antenna designs with accurate results for a wide range of antennas, substrates, superstrates, and superstrate spacings.

The resonant frequency model presented here, which includes an uncertainty analysis that incorporates the variability of electrical and geometric parameters, can be used to specify both electrical and physical design tolerances for integration of planar antennas into portable wireless equipment. The following section outlines the formulation of the model, including the filling fractions, effective microstrip line width, and effective permittivity of the resonant structure. Section III presents measurement and predicted resonant frequency data. Finally, Sections IV and V discuss the accuracy, uncertainty, and applicability of the new resonant frequency model.

II. Formulation

A. Effective Filling Fractions

The structure under investigation is shown in Fig. 1(a), with $w/h \geq 1$ (wide microstrip line), which is consistent with the configuration of a rectangular microstrip antenna with a dielectric superstrate. Svačina [16] conformally maps this three layer structure, including the dielectric boundaries, using Wheeler's [15] transformation from the physical z plane to the complex flux-potential g plane ($g = u + jv$). The degree of filling or filling fraction q_i of each of the dielectric materials in the g plane is defined by the ratio of the area occupied by each individual dielectric S_i (with $i = 1, 2, 3, \cdots$) and the entire area of the cross section S_C. These areas are depicted in Fig. 1(b). Svačina's equations for the filling fractions q_i are provided for reference as (1)–(3), with q_1, q_2, and q_3 equal to the effective filling fractions of the substrate dielectric (relative permittivity ε_{r1}), the superstrate dielectric (relative permittivity ε_{r2}), and the dielectric material above the superstrate (relative permittivity ε_{r3}), respectively

$$q_1 = \frac{S_1}{S_C} = 1 - \frac{h}{2w_{ef}} \ln\left(\frac{\pi}{h} w_{ef} - 1\right) \tag{1}$$

$$q_2 = \frac{S_2}{S_C} = 1 - q_1 - \frac{1}{2}\frac{h - v_\epsilon}{w_{ef}} \times \ln\left[\pi \frac{w_{ef}}{h} \frac{\cos\left(\frac{v_\epsilon}{2}\frac{\pi}{h}\right)}{\pi\left(\frac{h_2}{h} - \frac{1}{2}\right) + \frac{v_\epsilon}{2}\frac{\pi}{h}} + \sin\left(\frac{v_\epsilon}{2}\frac{\pi}{h}\right)\right] \tag{2}$$

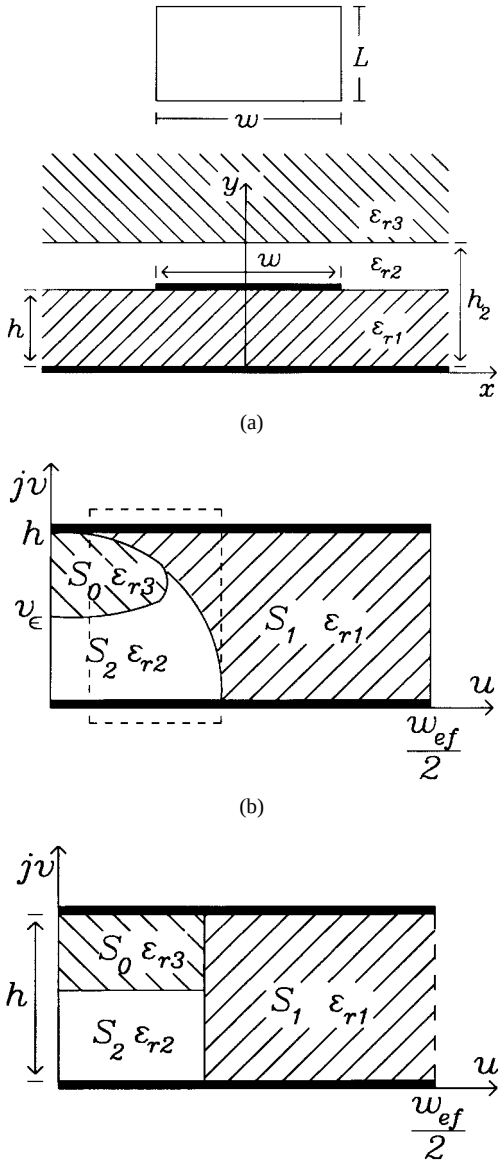

Fig. 1. (a) Top view and cross section of the general microstrip antenna structure under consideration. (b) Conformally mapped distribution of dielectric materials between equivalent parallel plate configuration with region of note enclosed by dotted line. (c) Approximate distribution of dielectric materials between parallel plates as presented in [16] and [17].

and

$$q_3 = \frac{1}{2}\frac{h - v_\epsilon}{w_{ef}} \times \ln\left[\pi \frac{w_{ef}}{h} \frac{\cos\left(\frac{v_\epsilon}{2}\frac{\pi}{h}\right)}{\pi\left(\frac{h_2}{h} - \frac{1}{2}\right) + \frac{v_\epsilon}{2}\frac{\pi}{h}} + \sin\left(\frac{v_\epsilon}{2}\frac{\pi}{h}\right)\right]. \tag{3}$$

Note that Svačina's filling fraction q_0 is denoted by q_3 in this discussion. This notation change reflects the more general results presented in this work for structures that have a spaced superstrate or a dielectric material other than air above a flush superstrate. In these equations, the effective line width w_{ef}

taken from [18] is

$$w_{ef} = w + \frac{2h}{\pi} \ln\left[17.08\left(\frac{w}{2h} + 0.92\right)\right] \tag{4}$$

and the quantity υ_ϵ is

$$\upsilon_\epsilon = \frac{2h}{\pi} \arctan\left[\frac{\pi}{\frac{\pi}{2}\frac{w_{ef}}{h} - 2}\left(\frac{h_2}{h} - 1\right)\right]. \tag{5}$$

Both [16] and [17] calculate the effective permittivity of the wide microstrip line based on the approximate capacitance of an equivalent parallel-plate structure with the filling fractions arranged as shown in Fig. 1(c) as

$$\varepsilon_{\text{eff}} = \varepsilon_{r1} q_1 + \varepsilon_{r2} \frac{(1 - q_1)^2}{\varepsilon_{r2}(1 - q_1 - q_2) + q_2} \tag{6}$$

assuming that the material above the flush superstrate has a relative permittivity equal to one. (Note that while Zhong's *et al.* [17] adaptation of Svačina's formulation addresses a microstrip structure with multilayer substrates in addition to superstrates, its application to the structure shown in Fig. 1(a) produces results identical to those given in [16].)

Both [16] and [17], however, ignore the behavior of the filling fraction expressions in the limit when there is no superstrate. In this case, $h_2 = h$, υ_ϵ goes to zero, and q_2 should also go to zero. However, q_2, as given in (2), does not go to zero in this limit, indicating that the models developed in both [16] and [17] overestimate the filling fraction of the superstrate (or the air gap in the case of a spaced superstrate) in all situations. We rectify this inconsistency by introducing a new filling fraction q_4 that is equal to half the value of q_2 in the limit when $h_2 = h$. Therefore

$$q_4 = \frac{h}{2w_{ef}} \ln\left(\frac{\pi}{2} - \frac{h}{2w_{ef}}\right). \tag{7}$$

Additionally, this new filling fraction is used to modify two of the existing filling fractions, with q_1(new) and q_2(new) now given by

$$\begin{aligned} q_1(\text{new}) &= q_1 - q_4 \\ q_2(\text{new}) &= 1 - q_1(\text{new}) - q_3 - 2q_4 \end{aligned} \tag{8}$$

with q_3 given by (3).

This alteration of filling fraction expressions more accurately reflects the distribution of dielectric materials as shown in Fig. 1(b). First, q_2(new) goes to zero in the limit when there is no superstrate ($h_2 = h$). Second, the creation of q_4 and the subsequent new expressions for q_1(new) and q_2(new) allow the model to include an important region of the conformal mapping that contains the substrate, air gap, and superstrate [indicated by dotted lines in Fig. 1(b)]. In this region, all three materials appear in series combinations between the equivalent parallel plates. The previously proposed filling fraction arrangement shown in Fig. 1(c) does not account for this region. Therefore, the new model utilizes q_4 to provide detail in a new dielectric distribution shown in Fig. 3 that accounts for these series combinations (discussed further in Section II-C). This analysis ignores the material above the spaced superstrate.

B. Effective Line Width

The expression for the effective line width (4) used in both [16] and [17] does not take the presence of the superstrate dielectric (flush or spaced) into account. The new methodology presented here utilizes a two-iteration procedure to calculate the new effective line width in the presence of a flush or spaced superstrate using the following equation derived from those presented in [15]

$$\begin{aligned} w_{ef} = &\sqrt{\frac{\varepsilon_r'}{\varepsilon_{\text{eff}}}}\left[w + 0.882h + 0.164\frac{h(\varepsilon_r' - 1)}{(\varepsilon_r')^2}\right] \\ &+ \sqrt{\frac{\varepsilon_r'}{\varepsilon_{\text{eff}}}}\frac{h(\varepsilon_r' + 1)}{\pi\varepsilon_r'}\left[\ln\left(\frac{w}{2h} + 0.94\right) + 1.451\right]. \end{aligned} \tag{9}$$

In (9), ε_r' is the relative permittivity of an ideal single-substrate microstrip structure that mimics the behavior of the actual multilayer structure under consideration. ε_r' is calculated using (11) presented in the next section. ε_{eff} is the composite effective permittivity of the multilayer structure.

As an approximation, the first iteration for w_{ef} assumes that $\varepsilon_r' \approx \varepsilon_{r1}$ and $\varepsilon_{\text{eff}} \approx \varepsilon_r'$. Once ε_{eff} and ε_r' are determined using this first value of w_{ef}, (9) is used to calculate the effective line width a second time. This new value of w_{ef} is used in the calculation of the effective open-line length extension ΔL. Our work indicates that additional iterations of this calculation loop result in insignificant changes in effective permittivity and predicted resonant frequency.

The adjusted set of filling fractions calculated with this new effective line width are next arranged between an equivalent parallel-plate capacitor configuration to obtain the effective permittivity of the microstrip structure shown in Fig. 1(a).

C. Effective Permittivity

In one of his classic papers on the subject, Wheeler [15] states that "... the conformal mapping of a boundary between two dielectrics is valid because it retains the angles of 'refraction' of the electric field at the boundary." However, characterization of multilayer dielectric structures requires more than correct mapping of the dielectric boundaries for the calculation of the effective permittivity of the structure. Specifically, the paths of the electric flux should be reflected as accurately as possible in the arrangement of the filling fractions between the conductors of the equivalent parallel-plate capacitor configuration.

Therefore, the arrangement of the new filling fractions within the equivalent parallel-plate structure is intended to represent the paths of electric field flux in the actual structure

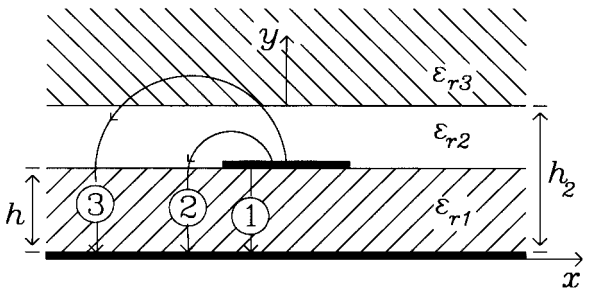

Fig. 2. Description of predominant electric flux paths present in a microstrip antenna structure with a flush or spaced dielectric superstrate.

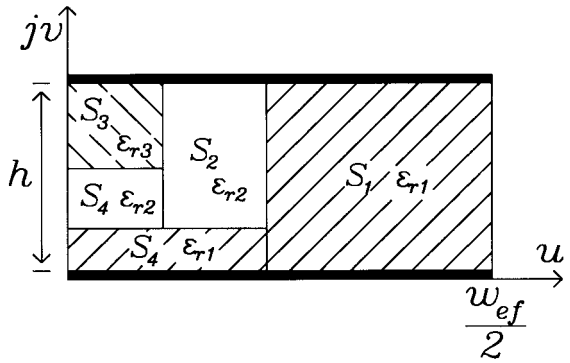

Fig. 3. Proposed filling fraction arrangement for calculation of effective permittivity that preserves the electric flux paths described in Fig. 2. The region to the extreme right (S_1, ε_{r2}) reproduces the capacitive effect of electric flux Path 1. The region containing $S_2(\varepsilon_{r2})$ and a portion of S_4 with relative permittivity equal to ε_{r1} reproduces the capacitive effect of electric flux Path 2. The remaining region to the extreme left containing $S_3(\varepsilon_{r3})$, $S_4(\varepsilon_{r2})$, and a portion of S_4 with relative permittivity equal to ε_{r1} reproduces the capacitive effect of electric flux Path 3.

as closely as possible. As shown in Fig. 2, the flux lines of the electric field can follow, in general, three different kinds of paths. Path 1 represents the flux that remains within the substrate of the structure. Path 2 represents the flux that exists strictly in the superstrate and substrate or, in the case of a spaced superstrate, the flux in the air gap and the substrate. Finally, Path 3 represents the flux lines that extend into the material above the superstrate or above the air gap. The previously proposed filling fraction arrangement shown in Fig. 1(c) does not account for the capacitive contributions of either Path 2 or Path 3. Preservation of the flux line paths results in the new filling fraction arrangement (with $q_i = S_i/S_C$ for each dielectric block) shown in Fig. 3. Derivation of the effective permittivity, ε_{eff}, of the equivalent parallel-plate structure depicted in Fig. 3 yields

$$\begin{aligned}\varepsilon_{\text{eff}} =& \varepsilon_{r1}q_1 + \varepsilon_{r1}(1-q_1)^2 \\ &\times [\varepsilon_{r2}^2 q_2 q_3 + \varepsilon_{r2}\varepsilon_{r3}(q_2 q_4 + (q_3+q_4)^2)] \\ &\times [\varepsilon_{r2}^2 q_2 q_3 q_4 + \varepsilon_{r1}(\varepsilon_{r2}q_3 + \varepsilon_{r3}q_4)(1-q_1-q_4)^2 \\ &+ \varepsilon_{r2}\varepsilon_{r3}q_4(q_2 q_4 + (q_3+q_4)^2)]^{-1}. \end{aligned} \tag{10}$$

This expression for the structure's effective permittivity can now be used to predict the resonant frequency of rectangular microstrip antennas with flush or spaced dielectric superstrates.

As noted in [17], calculation of the effective permittivity of the structure in Fig. 1(a) using (10) allows consideration of the structure as an equivalent microstrip configuration with a semi-infinite superstrate with relative permittivity equal to unity and a single dielectric substrate with relative permittivity equal to [19]

$$\varepsilon_r' = \frac{2\varepsilon_{\text{eff}} - 1 + A}{1 + A} \tag{11}$$

where

$$A = \left(1 + \frac{10h}{w_{ef}}\right)^{-1/2}. \tag{12}$$

Equation (12) is accurate within $\pm 2\%$ for all values of ε_r' [19].

D. Resonant Frequency

The resonant frequency of a rectangular microstrip antenna [shown in Fig. 1(a)] is given by [1]

$$f_r = \frac{c}{2(L + 2\Delta L)\sqrt{\varepsilon_{\text{eff}}}}$$

with c equal to the speed of light in vacuum, L equal to the length of the antenna, and ΔL equal to the effective open-line length extension. Following [17], the effective length extension ΔL is calculated using formulas presented in [20] with ε_r' given by (11) used in place of ε_r. As discussed in the previous section, the effective antenna width is calculated using (9). Since frequency dispersion in general decreases with increased conductor width in microstrip configurations, dispersion calculations were not included in this formulation. Zhong *et al.* [17] take dispersion into account using expressions given in [21]. Our investigation has shown that this procedure often results in a calculated resonant frequency that is more inaccurate than that calculated without accounting for dispersion.

III. Experimental Data

Several sets of measurements of rectangular patch antennas with flush and spaced superstrates are presented to test the accuracy of the resonant frequency model developed in Section II. In general, the resonant frequency is defined as the frequency at which the input impedance is purely real [22]. However, researchers commonly use either minimum return loss [12], [23] or maximum input resistance [24], [25] to indicate antenna resonance. In the case of microstrip antennas with substrate thicknesses less than $0.0815\lambda_o$ [25], measurements using the three resonant frequency definitions usually provide similar results. All of the antennas used in this study have thin substrates ($h < 0.0815\ \lambda_o$).

For antennas with flush superstrates, antenna dimensions and frequency measurements are taken from [12], which uses the minimum return loss specification of resonance. This data, as well as the calculated resonant frequencies using the present method and Zhong's *et al.* comparable closed-form model [17] are provided in Table I. Percentage errors use the measured resonant frequency as a reference.

For antennas with spaced superstrates, new resonant frequency measurements were performed using an HP 8753C

TABLE I
COMPARISON OF EXPERIMENTAL RESONANT FREQUENCIES FOR RECTANGULAR MICROSTRIP ANTENNAS WITH FLUSH SUPERSTRATES FROM [12] WITH PREDICTED VALUES OBTAINED WITH THE CLOSED-FORM MODELS PRESENTED IN [17] AND IN THIS WORK

Cover thickness $h_2 - h$ [mm]	f_r Exp. [GHz]	[17] Method f_r Calc. [GHz]	% Error	Present Method f_r Calc. [GHz]	% Error
3.18	3.104	3.111	0.22	3.098	0.20
6.36	3.025	3.092	2.23	3.077	1.72
9.54	2.980	3.078	3.30	3.064	2.83
12.72	2.955	3.067	3.80	3.056	3.42
L=28.5 mm, w=33.0 mm, h=3.18 mm, $\varepsilon_{r1} = \varepsilon_{r2} = 2.32$, ε_{r3} =1.0					

TABLE II
COMPARISON OF EXPERIMENTAL RESONANT FREQUENCIES, MINIMUM RETURN LOSS (S_{11}) FREQUENCIES, AND THEORETICALLY PREDICTED RESONANT FREQUENCIES FOR A RECTANGULAR MICROSTRIP ANTENNA WITH VARIOUS SPACED DIELECTRIC SUPERSTRATES. THE UNCOVERED ANTENNA RESONATED WITH A PURELY REAL INPUT IMPEDANCE AT 2.965 GHz. THE CALCULATED RESONANT FREQUENCY USES THE NOMINAL VALUES OF ALL ELECTRICAL AND GEOMETRIC PARAMETERS. THE RESONANT FREQUENCY UNCERTAINTY (Δf) IS CALCULATED USING THE APPROPRIATE PERMITTIVITY TOLERANCES AND THE FOLLOWING GEOMETRIC TOLERANCES: $\Delta L = \Delta w = \pm 0.02$ mm, $\Delta h = \pm 0.05$ mm, $\Delta(h_2 - h) = \pm 0.1$ mm

Air Gap $h_2 - h$ [mm]	ε_{r3}	Exp. [GHz] f_r	Exp. [GHz] f(min S_{11})	Present Method [GHz] f_r Calc.	Present Method [GHz] Δf
3.50	2.33 ± 0.02	2.940	2.935	2.937	±0.025
7.50	2.33 ± 0.02	2.931	2.938	2.946	±0.025
12.80	2.33 ± 0.02	2.948	2.947	2.952	±0.025
3.50	2.94 ± 0.04	2.949	2.939	2.930	±0.026
7.50	2.94 ± 0.04	2.940	2.940	2.943	±0.025
12.80	2.94 ± 0.04	2.954	2.948	2.951	±0.025
3.50	10.20 ± 0.25	2.922	2.926	2.891	±0.027
7.50	10.20 ± 0.25	2.905	2.932	2.925	±0.026
12.80	10.20 ± 0.25	2.954	2.943	2.944	±0.025
L=28.6 mm, w=36.7 mm, h=1.52 mm, ε_{r1} = 2.94 ± 0.04, ε_{r2} = 1.0					

vector network analyzer. For these cases, all of the antennas were probe-fed, with specific feed points determined using the procedure given in [26] for antennas with no superstrate present. Tables II and III present the antenna parameters, measured resonant frequencies (defined by purely real input impedances), measured minimum return loss (S_{11}) frequencies, and the results of predictions using the model developed here. Measured frequencies for minimum return loss (f(min S_{11})) differ from purely real input impedance frequencies (f_r) by less than 0.41% on average. Zhong's *et al.* [17] formulation is not used for comparison in Tables II and III since it does not explicitly account for spaced superstrates.

IV. DISCUSSION OF MODEL PERFORMANCE

The measured and predicted values of antenna resonant frequency presented in Tables I–III demonstrate the typical accuracy of the model presented here. In the case of flush superstrates, our model and that of [17] produce similar results with the added benefit of computational simplicity over many of the full wave analyses described in Section I. In the case of spaced superstrates, our method provides a high degree of accuracy. In general, cases involving a high permittivity superstrate exhibit slightly higher errors than those with low permittivity materials. The presence of a flush or spaced superstrate lowers the resonant frequency of the structure.

TABLE III
COMPARISON OF EXPERIMENTAL RESONANT FREQUENCIES, MINIMUM RETURN LOSS (S_{11}) FREQUENCIES, AND THEORETICALLY PREDICTED RESONANT FREQUENCIES FOR A RECTANGULAR MICROSTRIP ANTENNA WITH VARIOUS SPACED DIELECTRIC SUPERSTRATES. THE UNCOVERED ANTENNA RESONATED WITH PURELY REAL INPUT IMPEDANCE AT 3.508 GHz. THE CALCULATED RESONANT FREQUENCY USES THE NOMINAL VALUES OF ALL ELECTRICAL AND GEOMETRIC PARAMETERS. THE RESONANT FREQUENCY UNCERTAINTY (Δf) IS CALCULATED USING THE APPROPRIATE PERMITTIVITY TOLERANCES AND THE FOLLOWING GEOMETRIC TOLERANCES: $\Delta L = \Delta w = \pm 0.02$ mm, $\Delta h = \pm 0.1$ mm, $\Delta(h_2 - h) = \pm 0.1$ mm

Air Gap $h_2 - h$ [mm]	ε_{r3}	Exp. [GHz] f_r	Exp. [GHz] f(min S_{11})	Present Method [GHz] f_r Calc.	Present Method [GHz] Δf
3.50	2.33 ± 0.02	3.453	3.456	3.452	±0.036
7.50	2.33 ± 0.02	3.457	3.498	3.473	±0.035
12.80	2.33 ± 0.02	3.505	3.523	3.486	±0.035
3.50	2.94 ± 0.04	3.468	3.475	3.436	±0.036
7.50	2.94 ± 0.04	3.466	3.492	3.465	±0.035
12.80	2.94 ± 0.04	3.503	3.517	3.483	±0.035
3.50	10.20 ± 0.25	3.422	3.400	3.361	±0.039
7.50	10.20 ± 0.25	3.440	3.451	3.431	±0.036
12.80	10.20 ± 0.25	3.496	3.523	3.470	±0.035
L=22.7 mm, w=30.6 mm, h=3.05 mm, ε_{r1} = 2.94 ± 0.04, ε_{r2} = 1.0					

As discussed by several authors [1], [6], [24], the attainable accuracy of antenna design equations depends not only on the theoretical model but also on the tolerances of the electrical and geometric parameters of the antenna structure. Therefore, the range of possible predicted resonant frequencies in the case of rectangular patch antennas with flush and spaced super-

strates depends on the variability of the following parameters: h, h_2, ε_{r1}, ε_{r2}, ε_{r3}, L, and w. Mathematically

$$\Delta f_r = \frac{\partial f_r}{\partial h}\Delta h + \frac{\partial f_r}{\partial (h_2 - h)}\Delta(h_2 - h) + \frac{\partial f_r}{\partial \varepsilon_{r1}}\Delta\varepsilon_{r1} + \frac{\partial f_r}{\partial \varepsilon_{r2}}\Delta\varepsilon_{r2} + \frac{\partial f_r}{\partial \varepsilon_{r3}}\Delta\varepsilon_{r3} + \frac{\partial f_r}{\partial L}\Delta L + \frac{\partial f_r}{\partial w}\Delta w. \tag{13}$$

While explicit symbolic analysis of (13) is rather complicated, the closed-form model lends itself well to the determination of resonant frequency uncertainties for a given set of electrical and geometric tolerances. The uncertainty in each resonant frequency calculation is presented in Tables II and III for each antenna configuration, using appropriate permittivity and geometric tolerances as noted.

This formulation is broadly applicable to rectangular microstrip antenna designs that use thin $(h < 0.0815\lambda_o)$ [25], low permittivity $(\varepsilon_{r1} < 3)$ substrates. While most microstrip antenna designs satisfy these conditions, the model does not address explicitly the following situations. First, the model does not account for surface wave losses arising from high permittivity substrates and superstrates [27]. Second, the model does not account for nonideal feed conditions caused by electrically thick substrates $(h > 0.0815\lambda_o)$ [24], [28]. Finally, the model is not applicable at very high frequencies where the assumption of TEM mode propagation in the microstrip structure is invalid [15].

V. Conclusion

This paper presents a predictive model for the resonant frequencies of rectangular microstrip antennas with flush and spaced superstrates. The development of new filling fractions rectifies inconsistencies in previous work and supports a new arrangement of these filling fractions that reflects the true configuration of the electric flux in the multilayer structure. This closed-form model is suitable for CAD and is directly applicable for the integration of microstrip antennas beneath plastic covers or protective dielectric superstrates in portable wireless equipment. Additionally, the model can be used to specify both electrical and geometric tolerances during the design process. A comparison between calculated and measured resonant frequencies demonstrates that the model provides less than 1% errors on average for structures containing materials with low relative permittivities ($\varepsilon_r < 3$) and slightly higher errors for structures that contain higher permittivity materials. Generally, the model predicts the resonant frequency of a spaced superstrate structure as accurately as possible within the tolerance range of the structure's electrical and geometric parameters.

Acknowledgment

The authors would like to thank the reviewers for their helpful comments and suggestions. They would also like to thank the Rogers Corporation, Chandler, AZ, for providing the dielectric substrate material for this work.

References

[1] I. J. Bahl, P. Bhartia, and S. Stuchly, "Design of microstrip antennas covered with a dielectric layer," *IEEE Trans. Antennas Propagat.*, vol. 30, pp. 314–318, Mar. 1982.
[2] A. K. Verma, A. Bhupal, Z. Rostamy, and G. P. Srivastava, "Analysis of rectangular patch antenna with dielectric cover," *IEICE Trans.*, vol. E74, pp. 1270–1276, May 1991.
[3] R. Shavit, "Dielectric cover effect on rectangular microstrip antenna array," *IEEE Trans. Antennas Propagat.*, vol. 42, pp. 1180–1184, Aug. 1994.
[4] Z. Fan and K. F. Lee, "Input impedance of annular-ring microstrip antenna with a dielectric cover," *IEEE Trans. Antennas Propagat.*, vol. 40, pp. 992–995, Aug. 1992.
[5] A. Verma and Z. Rostamy, "Resonant frequency of uncovered and covered rectangular microstrip patch using modified Wolff model," *IEEE Trans. Microwave Theory Tech.*, vol. 41, pp. 109–116, Jan. 1993.
[6] J. P. Damiano and A. Papiernik, "A simple and accurate model for the resonant frequency and the input impedance of printed antennas," *Int. J. Microwave Millimeter-Wave Computer-Aided Eng.*, vol. 3, pp. 350–361, 1993.
[7] J. P. Damiano, J. M. Rivero, and R. Staraj, "Original simple and accurate model for elliptical microstrip antennas," *Electron. Lett.*, vol. 31, pp. 1023–1024, June 1995.
[8] D. M. Pozar, "Input impedance and mutual coupling of rectangular microstrip antennas," *IEEE Trans. Antennas Propagat.*, vol. 30, pp. 1191–1196, Nov. 1982.
[9] J. R. Mosig and F. E. Gardiol, "General integral equation formulation for microstrip antennas and scatterers," *Proc. Inst. Elect. Eng.*, vol. 132, pt. H, pp. 424–432, Dec. 1985.
[10] K. A. Michalski and D. Zheng, "Analysis of microstrip resonators of arbitrary shape," *IEEE Trans. Microwave Theory Tech.*, vol. 40, pp. 112–119, Jan. 1992.
[11] O. M. Ramahi and Y. T. Lo, "Superstrate effect on the resonant frequency of microstrip antennas," *Microwave Opt. Technol. Lett.*, vol. 5, pp. 254–257, June 1992.
[12] A. Bhattacharyya and T. Tralman, "Effects of dielectric superstrate on patch antennas," *Electron. Lett.*, vol. 24, pp. 356–358, Mar. 1988.
[13] R. Afzalzadeh and R. N. Karekar, "Characteristics of a rectangular microstrip patch antenna with protecting spaced dielectric superstrate," *Microwave Opt. Technol. Lett.*, vol. 7, pp. 62–66, Feb. 1994.
[14] D. M. Pozar, "Microstrip antennas," *Proc. IEEE*, vol. 80, pp. 79–91, Jan. 1992.
[15] H. A. Wheeler, "Transmission-line properties of parallel strips separated by a dielectric sheet," *IEEE Trans. Microwave Theory Tech.*, vol. 13, pp. 172–185, Mar. 1965.
[16] J. Svačina, "Analysis of multilayer microstrip lines by a conformal mapping method," *IEEE Trans. Microwave Theory Tech.*, vol. 40, pp. 769–772, Apr. 1992.
[17] S.-S. Zhong, G. Liu, and G. Qasim, "Closed form expressions for resonant frequency of rectangular patch antennas with multidielectric layers," *IEEE Trans. Antennas Propagat.*, vol. 42, pp. 1360–1363, Sept. 1994.
[18] H. Wheeler, "Transmission-line properties of parallel wide strips by a conformal mapping approximation," *IEEE Trans. Microwave Theory Tech.*, vol. 12, pp. 280–289, Mar. 1964.
[19] M. V. Schneider, "Microstrip lines for microwave integrated circuits," *Bell Syst. Tech. J.*, vol. 48, pp. 1421–1443, May/June 1969.
[20] M. Kirschning, R. H. Jansen, and N. H. L. Koster, "Accurate model for open end effect of microstrip lines," *Electron. Lett.*, vol. 17, pp. 123–125, Feb. 1981.
[21] M. Kirschning and R. H. Jansen, "Accurate model for effective dielectric constant of microstrip with validity up to millimeter-wave frequencies," *Electron. Lett.*, vol. 18, pp. 272–273, Mar. 1982.
[22] S. Ramo, J. R. Whinnery, and T. V. Duzer, *Fields and Waves in Communication Electronics*, 3rd ed. New York: Wiley, 1994.
[23] S. H. Al-Charchafchi and M. R. Ibrahim, "An experimental investigation of flat radome-loaded microstrip patch antennas," *Microwave J.*, vol. 40, pp. 100–109, Feb. 1997.
[24] R. W. Dearnley and A. R. F. Barel, "A comparison of models to determine the resonant frequencies of a rectangular microstrip antenna," *IEEE Trans. Antennas Propagat.*, vol. 37, pp. 114–118, Jan. 1989.
[25] M. Kara, "Closed-form expressions for the resonant frequency of rectangular microstrip antenna elements with thick substrates," *Microwave Opt. Technol. Lett.*, vol. 12, pp. 131–136, June 1996.
[26] I. J. Bahl and P. Bhartia, *Microstrip Antennas*. Dedham, MA: Artech House, 1980.
[27] D. M. Pozar, "Rigorous closed-form expressions for the surface wave

loss of printed antennas," *Electron. Lett.*, vol. 26, pp. 954–956, June 1990.

[28] M. Kara, "Empirical formulas for the computation of the physical properties of rectangular microstrip antenna elements with thick substrates," *Microwave Opt. Technol. Lett.*, vol. 14, pp. 115–121, Feb. 1997.

Jennifer T. Bernhard (S'89–M'94) was born in New Hartford, NY, on May 1, 1966. She received the B.S.E.E. degree from Cornell University, Ithaca, NY, in 1988, and the M.S. and Ph.D. degrees from Duke University, Durham, NC, in 1990 and 1994, respectively.

From 1986 to 1988, she participated in Cornell's Engineering Co-op Program, working at IBM Federal Systems Division, Owego, NY. During the 1994–1995 academic year she held the position of Postdoctoral Research Associate with the Departments of Radiation Oncology and Electrical Engineering, Duke University. Over the past five years she has also worked as a consultant on antennas and wireless communication systems. Since 1995 she has been an Assistant Professor of Electrical Engineering at the University of New Hampshire (UNH), Durham. For the 1998–1999 academic year, she is on leave as a Visiting Assistant Professor with the Electromagnetics Laboratory at the University of Illinois, Urbana-Champaign. Her research interests are in the areas of high-speed wireless data communication, microwave antennas and circuits, electromagnetic compatibility, and electromagnetics for industrial and medical applications.

Dr. Bernhard received the 1997–1998 Teaching Excellence Award for the College of Engineering and Physical Sciences at UNH. She is a member of Tau Beta Pi, Eta Kappa Nu, and Sigma Xi. She received a National Science Foundation Graduate Fellowship for her studies at Duke University.

Carolyn J. Tousignant (S'93–M'98) was born in Concord, NH, on December 13, 1964. She received the B.S.E.E. degree from the University of New Hampshire (UNH), Durham, in 1997. She is currently working toward the M.S.E.E. degree at the same university.

From 1983 to 1992, she was in the U.S. Air Force, attaining the rank of Staff Sergeant and working as an Emitter Location and Identification Systems Supervisor. In 1997, she joined Raytheon Systems Company as a member of the technical staff. Her work has focused on low noise exciters and receivers for missile applications. She continues to be an active member of the New Hampshire Air National Guard as an avionics technician on KC-135R aircraft.

Ms. Tousignant participated in the Electrical and Computer Engineering Department's NSF Research Experience for Undergraduates program and was chair of the Student Branch of the IEEE from 1996 to 1997 during her undergraduate studies.